J. Fluid Mech. (1983), *vol.* 128, *pp.* 155–180
Printed in Great Britain

Surface-wave diffraction by a periodic row of submerged ducts

By JOHN W. MILES
Institute of Geophysics and Planetary Physics, University of California, San Diego

(Received 24 May 1982 and in revised form 24 September 1982)

The diffraction of a gravity wave of length λ that is obliquely incident upon, and the radiation from, a periodic row of vertical circular ducts of radii a and horizontal spacing b with mouths at a distance h below the free surface of a deep ocean are determined through integral-equation and variational formulations. Numerical results for the reflection coefficient, the pressure-amplification factor (the ratio of the complex amplitude of the wave-induced pressure in the depths of the duct to that of the incident wave at the level of the mouths), and the radiation impedance (the real and imaginary parts of which are measures of the radiation damping and the virtual mass or stiffness of the fluid external to the ducts) are presented as functions of a/λ with a/b and a/h as parameters for the special case of normal incidence with $\lambda > b$ (which implies that the crests of the scattered waves are parallel to the midplane of the ducts). These results, which complement those of Simon (1981) for a single duct, are of practical interest for wave-power absorption.

1. Introduction

I consider here (i) the diffraction of a surface wave of angular frequency ω and length $\lambda = 2\pi g/\omega^2$ that is obliquely incident upon, and (ii) the radiation of such a wave from, a row of vertical circular ducts of radii a and horizontal (periodic) spacing b with open mouths at depth h (figure 1). The problem of an isolated duct has been considered by Simon (1981), Thomas (1981)† and Miles (1982*a*). Measurements for a duct in both 'narrow' ($b < \lambda$) and 'wide' ($b \gg \lambda$) wave tanks have been made by Knott & Flower (1980). These papers also describe the practical significance of the problem; see Lighthill (1979) for further background on the duct problem and Evans (1981) for a review of the general problem of wave-power absorption. The diffraction problem for $h < 0$ (duct penetrates free surface) is equivalent to that for acoustical diffraction by a periodic grating of circular cylinders, which has a long history and for which rather extensive analytical results are available (Twersky 1962). It should be emphasized, however, that the limit $h \downarrow 0$ is singular and that the primary reason for considering $h < 0$ in the present context is that the solution of that simpler problem is an essential component of the solution for $h > 0$.

I ultimately assume normal incidence and $b < \lambda$, for which the problem is equivalent to that of a single duct midway between the walls of a deep wave tank of width b in which only the dominant mode is propagated. The scattered field then comprises only the transmitted and reflected counterparts of the incident wave, and

† Thomas assumes finite depth, which implies a discrete spectrum for the vertical wavenumber, whereas the spectrum for the deep-water problem comprises a single discrete eigenvalue for the surface wave and a continuous spectrum for the non-propagated internal waves. The deep-water approximation appears to be adequate for practical configurations.

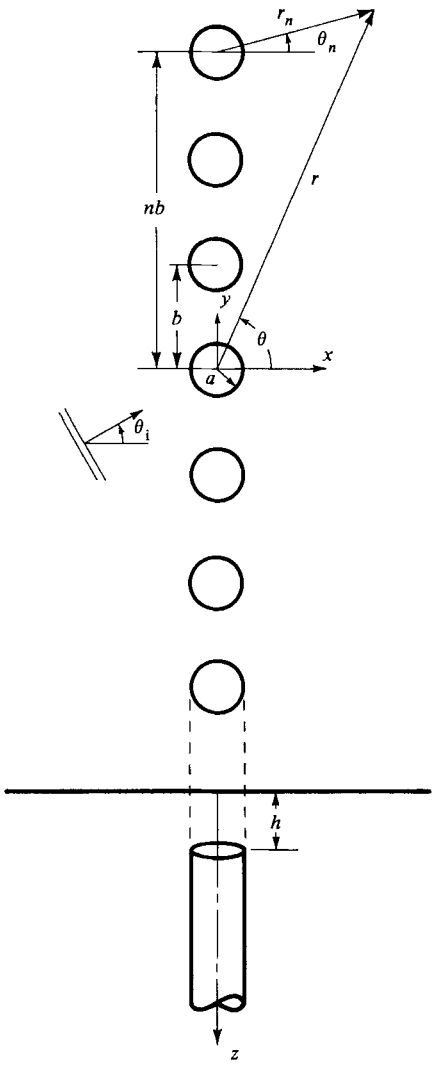

FIGURE 1. Plan and elevation of periodic row of circular ducts in deep ocean.

my results complement those of Simon and are comparable with the measurements in Knott & Flower's narrow tank. The restriction $b < \lambda$ precludes the direct transition between the present results and those of Simon; however, Simon's results may be obtained from the present results by retaining only the $n = 0$ terms in (2.15) and (2.18) below and renormalizing the subsequent calculations (see §8).

I begin the solution of the diffraction problem in §2 by using Green's theorem to express the solution in terms of the pressure jumps across the walls of the ducts. I then introduce Havelock's (1929) Fourier transformation with respect to the vertical coordinate in §3 and construct the Green function in §4.† The formulation to this

† The procedure adopted in §§2 and 4 follows that for the simpler (no z-dependence) problem of acoustical scattering (cf. Twersky 1962); see also Falnes & Budal (1982). An alternative procedure for $b \gg \lambda$ would be to perturb the solution for a single duct by invoking the Born approximation (or hierarchy of approximations) for multiple scattering by a widely spaced array of scatters; cf. Simon (1982) and references therein.

point is valid for arbitrary angle of incidence and duct spacing. Practical computation requires further simplification, and in §5 I impose the restrictions of normal incidence and $b < \lambda$. (The generalization of §§5–8 for oblique incidence and arbitrary spacing is straightforward in principle but complicated in detail.) I then separate the solution into symmetric and antisymmetric (with respect to a transverse plane through the axes of the ducts) components and construct a pair of real integral equations for the corresponding components of the pressure jump. In §§6 ($h < 0$) and 7 ($h > 0$) I construct variational approximations to a pair of real parameters that represent the symmetric and antisymmetric components of the solution and from which the complex reflexion and transmission coefficients may be calculated. In §8 I calculate the pressure-amplification factor for the duct, defined as the ratio of the complex amplitude of the wave-induced pressure in the depths of the duct to that of the incident wave at the centre of the mouth.

Finally, in §9 I formulate the radiation problem for a duct in a wave tank (or, equivalently, a periodic row of ducts for which the forcing motions are in phase) wherein the motion is excited by an oscillating piston in the depths of the duct. The solution then is symmetric but nevertheless is governed by a pair of real integral equations (cf. Miles 1982*a*). One of these integral equations is equivalent to that for the symmetric scattering problem; the other has a similar structure. The parameters of principal interest for the radiation problem are the amplitude of the radiated wave and the radiation impedance (the ratio of the complex amplitude of the pressure to that of the velocity in the depths of the duct less the corresponding ratio for the column of water in $r < a$, regarded independently of the water in $r > a$). Both the amplitude of the radiated wave and the radiation resistance may be expressed in terms of the pressure-amplification factor for the diffraction problem through generalizations of Simon's (1981) reciprocal theorems for the single duct. The procedure used by Simon to obtain the radiation reactance is not applicable in the present problem, however, and I determine it by solving the second of the aforementioned integral equations.

2. The diffraction problem

The deep-water gravity wave described by the velocity potential

$$\phi(\mathbf{r}, z, t) = \frac{g}{\omega} \operatorname{Re}\{iA\, e^{i(\omega t - \boldsymbol{\kappa}.\mathbf{r}) - \kappa z}\}, \quad \mathbf{r} = (x, y) = r(\cos\theta, \sin\theta), \tag{2.1a,b}$$

where A is the complex amplitude of the free-surface displacement, ω is the angular frequency,

$$\boldsymbol{\kappa} = \kappa(\cos\theta_i, \sin\theta_i), \quad \kappa \equiv \frac{2\pi}{\lambda} = \frac{\omega^2}{g}, \tag{2.2a,b}$$

and θ_i is the angle of incidence, is incident upon a periodic row of semi-infinite circular ducts (figure 1) of radii a with axes at $x = 0$ and $y = nb$ ($n = 0, \pm 1, \pm 2, \ldots$) and open mouths at $z = h$ in a semi-infinite ocean ($0 < z < \infty$). The resulting perturbation pressure may be posed in the form

$$p(\mathbf{r}, z, t) = \rho g \operatorname{Re}\{A\, e^{i\omega t}\, \psi(\mathbf{r}, z)\}, \tag{2.3}$$

where ρ is the density (but ρ appears as a radius in the subsequent development), and the dimensionless, complex pressure ψ satisfies Laplace's equation,

$$\nabla^2 \psi = 0. \tag{2.4}$$

The boundary conditions at the free surface, the (infinitely remote) bottom and the walls of the ducts imply

$$(\partial_z+\kappa)\psi = 0 \quad (z = 0), \quad \lim_{z\to\infty} \partial_z\psi = 0, \tag{2.5a,b}$$

$$\partial_{r_n}\psi = 0 \quad (r_n = a, \quad n = 0, \pm 1, \pm 2, \ldots), \tag{2.6}$$

where

$$\mathbf{r}_n = \mathbf{r} - n\mathbf{b} \equiv r_n(\cos\theta_n, \sin\theta_n), \quad \mathbf{b} = (0, b). \tag{2.7a,b}$$

It follows from (2.1) and (2.3) that the incident wave is described by

$$\psi^{\mathrm{i}}(\mathbf{r}, z; \theta_{\mathrm{i}}) = e^{-i\boldsymbol{\kappa}.\mathbf{r}-\kappa z} = e^{-i\kappa(x\cos\theta_{\mathrm{i}}+y\sin\theta_{\mathrm{i}})-\kappa z}, \tag{2.8}$$

which satisfies (2.4) and (2.5a,b). Substituting $\mathbf{r} = \mathbf{r}_n + n\mathbf{b}$ into (2.8), we obtain

$$\psi^{\mathrm{i}} = e^{-in\beta}e^{-i\boldsymbol{\kappa}.\mathbf{r}_n-\kappa z}, \quad \beta = \boldsymbol{\kappa}.\mathbf{b} = \kappa b\sin\theta_{\mathrm{i}}, \tag{2.9a,b}$$

which exhibits the interduct phase shift β associated with the inclination of the incident wave crests to the midplane of the ducts.

The scattered wave may be expressed in terms of the (dimensionless) pressure jumps across the duct walls,

$$\chi_n \equiv \psi|_{r_n=a-} - \psi|_{r_n=a+} \tag{2.10}$$

(note that $\chi_n = 0$ in $0 \leqslant z \leqslant h$, in which interval ψ must be continuous across $r = a$), with the aid of Green's second identity,

$$\int\int\int (G\nabla^2\psi - \psi\nabla^2 G)\, d\xi\, d\eta\, d\zeta = \int\int (\psi\,\partial_\nu G - G\,\partial_\nu\psi)\, dS, \tag{2.11}$$

where the Green function G satisfies

$$\nabla^2 G(\mathbf{r}, z; \boldsymbol{\rho}, \zeta) = -\delta(\mathbf{r}-\boldsymbol{\rho})\,\delta(z-\zeta), \tag{2.12}$$

the counterparts of (2.5a,b), and appropriate finiteness and radiation conditions as $r \to \infty$; δ is Dirac's delta function; the semi-infinite domain of integration is bounded externally by $\zeta = 0$ and internally by the duct walls; the Laplacian ∇^2 operates on

$$\boldsymbol{\rho} \equiv (\xi, \eta) \equiv \rho(\cos\alpha, \sin\alpha) \tag{2.13}$$

and ζ in the integrands in (2.11) and on $\mathbf{r}$ and z in (2.12); ν is the inwardly directed normal to the bounding surface, and dS is an element of that surface. It follows from (2.9) and linearity that

$$\chi_n(\theta, z) = e^{-in\beta}\chi(\theta_n, z), \tag{2.14}$$

where $\chi(\theta, z)$ is the pressure jump across the wall of the central duct. Substituting (2.14) into (2.11) and invoking (2.4), (2.12) and the corresponding boundary conditions, we obtain the total (incident plus scattered) field in the form

$$\psi = \psi^{\mathrm{i}} - \int_D \chi(\alpha, \zeta)\,\partial_\rho \sum_n e^{-in\beta} G(\mathbf{r}, z; \boldsymbol{\rho} + n\mathbf{b}, \zeta)\, dS, \tag{2.15}$$

where

$$\int_D (\;)\, dS \equiv \int_0^{2\pi}\int_h^\infty (\;)\, a\, d\alpha\, d\zeta, \tag{2.16}$$

the summation is over $-\infty$ to ∞ (as are all subsequent summations except as explicitly indicated), and it is implicit that $\rho = a$ after carrying out the differentiation with respect to ρ.

It follows from (2.9) and (2.15) that $\exp(in\beta)\psi(y-nb) = \psi(y)$ for $n = 0, \pm 1 \ldots$ (this statement anticipates that $G(\mathbf{r}, z; \boldsymbol{\rho}, \zeta)$ is a function of $\mathbf{r}-\boldsymbol{\rho}$, rather than $\mathbf{r}$ and

$\boldsymbol{\rho}$ separately); accordingly, it suffices to impose the boundary condition (2.6) on the central ($n = 0$) duct.† This yields the integral equation

$$\partial_r \psi^{\mathrm{i}} + \int_D \chi(\alpha, \zeta)\, K(\theta, z; \alpha, \zeta)\, dS = 0 \quad (z > h), \tag{2.17}$$

where

$$K = -\partial_r \partial_\rho \sum_n e^{-in\beta}\, G(\mathbf{r}, z; \boldsymbol{\rho} + n\mathbf{b}, \zeta), \tag{2.18}$$

and it is implicit that $r = \rho = a$ after carrying out the differentiations with respect to r and ρ. We anticipate that (2.17) can be separated into a pair of uncoupled integral equations governing the symmetric and antisymmetric components of χ:

$$\chi_{\mathrm{s,a}}(\theta, z) = \tfrac{1}{2}\{\chi(\theta, z) \pm \chi(\pi - \theta, z)\}, \tag{2.19}$$

where, here and subsequently, the upper/lower choice of alternative signs corresponds to the symmetric/antisymmetric component.

3. Fourier transformation

The functions

$$Z_k(z) = \cos kz - \frac{\kappa}{k} \sin kz \tag{3.1}$$

form a complete set for the interval $0 < z < \infty$ with the end conditions (2.5a, b), which imply the discrete spectrum $k = \pm i\kappa$ (these eigenvalues correspond to surface waves) and the continuous spectrum $0 < k < \infty$. The corresponding Fourier-transform pair is given by (cf. Havelock 1929)

$$F(k) = \int_0^\infty f(z)\, Z_k(z)\, dz \equiv \mathbf{F}\{f(z)\}, \tag{3.2}$$

$$f(z) = 2\kappa F(i\kappa)\, Z_{i\kappa}(z) + \frac{2}{\pi} \int_0^\infty F(k)\, Z_k(z)\, \frac{k^2\, dk}{k^2 + \kappa^2} \equiv \mathbf{F}^{-1}\{F(k)\}, \tag{3.3}$$

which provides the basis for the solution of either (2.4) or (2.12) and (2.5) through separation of variables. Note that Z_k and F are even functions of k and that

$$Z_{i\kappa}(z) = Z_{-i\kappa}(z) = e^{-\kappa z}. \tag{3.4}$$

4. Green function

Multiplying (2.12) through by $Z_k(z)$, integrating from $z = 0$ to $z = \infty$ as in (3.2), integrating $Z_k\, \partial_z^2 G$ by parts, invoking the boundary conditions (2.5), and introducing

$$\mathbf{G}(\mathbf{r}; \boldsymbol{\rho}; k) \equiv \{Z_k(\zeta)\}^{-1} \mathbf{F}\{G(\mathbf{r}, z; \boldsymbol{\rho}, \zeta)\}, \tag{4.1}$$

we obtain

$$(\nabla^2 - k^2)\, \mathbf{G}(\mathbf{r}; \boldsymbol{\rho}; k) = -\delta(\mathbf{r} - \boldsymbol{\rho}), \tag{4.2}$$

wherein the Laplacian ∇^2 operates on $\mathbf{r}$. The solution of (4.2), subject to finiteness and radiation conditions as $r \to \infty$, is given by

$$\mathbf{G}(\mathbf{r}; \boldsymbol{\rho}; k) = (2\pi)^{-1} K_0(k|\mathbf{r} - \boldsymbol{\rho}|) \quad (\mathrm{Re}\, k \geqslant 0) \tag{4.3a}$$

$$= -\tfrac{1}{4} i H_0^{(2)}(\kappa|\mathbf{r} - \boldsymbol{\rho}|) \quad (k = i\kappa), \tag{4.3b}$$

† If (2.6) were invoked at the Nth duct the counterpart of (2.17) could be multiplied through by $\exp(iN\beta)$, (2.9) invoked, and the summation index in (2.18) replaced by $n - N$ to recover (2.17).

where K_0 is a modified Bessel function and $H_0^{(2)}$ is a Hankel function. Note that the choice $k = i\kappa$, rather than $k = -i\kappa$, in (4.3*b*) is dictated by the radiation condition at $r = \infty$ in conjunction with the time dependence $\exp(i\omega t)$.

The explicit representation of the kernel K, obtained through the substitution of the inverse transform of (4.1) into (2.18), requires that $K_0(k|\mathbf{r}-\boldsymbol{\rho}-n\mathbf{b}|)$ be expressed as a function of r, θ, ρ and α. Remarking that $\mathbf{r}-\boldsymbol{\rho}-n\mathbf{b} = \mathbf{r}_n-\boldsymbol{\rho}$, invoking the addition theorems (Watson 1945, §11.3(8))

$$K_0(k|\mathbf{r}_n-\boldsymbol{\rho}|) = \sum_m I_m(k\rho)\, K_m(kr_n)\, e^{im(\theta_n-\alpha)} \quad (\rho \leqslant r_n), \tag{4.4}$$

in which ρ and r_n must be reversed if $\rho > r_n$, and (for a triangle with sides r, r_n and $|n|\,b$)

$$K_m(kr_n)\exp\{im(\tfrac{1}{2}\pi\,\operatorname{sgn} n+\theta_n)\}$$
$$= \sum_l I_l(kr)\, K_{l+m}(|n|\,kb)\exp\{il(\tfrac{1}{2}\pi\,\operatorname{sgn} n-\theta)\} \quad (r < |n|\,b), \tag{4.5}$$

using (4.4) for $n = 0$, and combining (4.4) and (4.5) for $n = \pm 1, \pm 2, \ldots$, we obtain

$$\mathbf{K}(\theta;\alpha;k) \equiv \{Z_k(\zeta)\}^{-1}\mathbf{F}K(\theta,z;\alpha,\zeta)$$
$$= -\frac{k^2}{2\pi}\Bigg[\sum_m I'_m(ka)\, K'_m(ka)\, e^{im(\theta-\alpha)} + 2\sum_l\sum_m I'_l(ka)\, I'_m(ka)\, e^{-i(l\theta+m\alpha)}$$
$$\times \sum_{n=1}^{\infty} K_{l+m}(nkb)\cos\{(l-m)\tfrac{1}{2}\pi - n\beta\}\Bigg]. \tag{4.6}$$

This representation may be separated into the sum of symmetrical and antisymmetrical components, which are respectively even and odd functions of each of $\frac{1}{2}\pi+\theta$ and $\frac{1}{2}\pi+\alpha$, as anticipated in §2.

The calculation of the scattered field is facilitated by a plane-wave (where *wave* now implies either a propagated or a non-propagated wave) representation of

$\sum_n \exp(-in\beta)\, G(\mathbf{r},z;\boldsymbol{\rho}+n\mathbf{b},\zeta)$ in preference to the cylindrical wave representation implied by (4.3)–(4.5). This may be achieved with the aid of the integral representation (Magnus, Oberhettinger & Soni 1966, p. 86)

$$K_0\{(x^2+y^2)^{\frac{1}{2}}\} = \frac{1}{2}\int_{-\infty}^{\infty} e^{-|x|\cosh t + iy\sinh t}\, dt. \tag{4.7}$$

Substituting (4.7) into (4.3*a*) after replacing x and y by $k|x-\xi|$ and $k(y-nb-\eta)$, effecting the change of variable $\tau = k\sinh t$ with the provisional restriction $k > 0$, multiplying the result by $\exp(-in\beta)$, and summing over n, we obtain

$$\sum_n e^{-in\beta}\,\mathbf{G}(\mathbf{r};\boldsymbol{\rho}+n\mathbf{b};k)$$
$$= (4\pi)^{-1}\int_{-\infty}^{\infty} \exp\{-(k^2+\tau^2)^{\frac{1}{2}}|x-\xi| + i\tau(y-\eta)\}\,\boldsymbol{\Sigma}(\tau)\,(k^2+\tau^2)^{-\frac{1}{2}}\,d\tau, \tag{4.8}$$

where (after substituting $\beta = \kappa b\sin\theta_i$)

$$\boldsymbol{\Sigma}(\tau) = \sum_n e^{-inb(\tau+\kappa\sin\theta_i)}. \tag{4.9}$$

Invoking the transformation (which is equivalent to Fourier's theorem)

$$\Sigma(\tau) = \frac{2\pi}{b} \sum_m \delta(\tau - \nu_m), \quad \nu_m = 2\pi m b^{-1} - \kappa \sin\theta_i, \tag{4.10a,b}$$

and carrying out the integration with respect to τ in (4.8), we obtain

$$\sum_n e^{-in\beta} \mathbf{G}(\mathbf{r}; \boldsymbol{\rho} + n\mathbf{b}; k) = (2b)^{-1} \sum_m (k^2 + \nu_m^2)^{-\frac{1}{2}} \exp\{-(k^2+\nu_m^2)^{\frac{1}{2}} |x-\xi| + i\nu_m(y-\eta)\}. \tag{4.11}$$

The inverse transform $\mathbf{F}^{-1}\{(4.11)\, Z_k(\zeta)\}$, as given by (4.1) and (3.3), comprises a continuous spectrum ($0 < k < \infty$) of trapped (by the periodic row of ducts) waves and a discrete spectrum ($k = i\kappa$) of an infinite number of trapped waves, for which $|\nu_m| > \kappa$, plus a finite number of propagated waves, for which $|\nu_m| < \kappa$; only the latter appear in the scattered field. Setting $k = i\kappa$ in (4.11), introducing

$$\sin\theta_m \equiv -\frac{\nu_m}{\kappa} = \sin\theta_i - \frac{m\lambda}{b} \tag{4.12}$$

(note that the θ_n defined by (2.7) do not appear in the subsequent development), choosing $(\nu_m^2 - \kappa^2)^{\frac{1}{2}} = i\kappa \cos\theta_m$ (in satisfaction of the radiation condition at $x = \pm\infty$), and invoking (3.3) and (3.4), we obtain

$$\sum_n e^{-in\beta} G(\mathbf{r}, z; \boldsymbol{\rho} + n\mathbf{b}, \zeta)$$

$$\sim 2\kappa e^{-\kappa z} \sum_n e^{-in\beta} \mathbf{G}(\mathbf{r}; \boldsymbol{\rho} + n\mathbf{b}; i\kappa)\, e^{-\kappa\zeta} \tag{4.13a}$$

$$\sim e^{-\kappa(z+\zeta)} \sum_m (ib\cos\theta_m)^{-1} \exp[-i\kappa\{|x-\xi|\cos\theta_m + (y-\eta)\sin\theta_m\}] \quad (|x-\xi| \to \infty), \tag{4.13b}$$

$$= \sum_m (ib\cos\theta_m)^{-1} \psi^i\left(\mathbf{r}, z; \begin{matrix}\theta_m \\ \pi - \theta_m\end{matrix}\right) \psi^{i*}\left(\boldsymbol{\rho}, \zeta, \begin{matrix}\theta_m \\ \pi - \theta_m\end{matrix}\right) \quad (x \to \pm\infty), \tag{4.13c}$$

where ψ^i and ψ^{i*} are given by (2.8) and its complex conjugate, and the summations in (4.13*b*, *c*) are only over those m for which θ_m is real.

If, as we now and subsequently assume, $b(1 + |\sin\theta_i|) < \lambda$, only the dominant ($m = 0$) mode is propagated, and the substitution of (4.13*c*) into (2.15) yields

$$\psi \sim \begin{cases} T\psi^i(\theta_i) & (x \to +\infty), \\ \psi^i(\theta_i) + R\psi^i(\pi - \theta_i) & (x \to -\infty), \end{cases} \tag{4.14}$$

where

$$T = 1 + i(b\cos\theta_i)^{-1} \partial_\rho \int_D \chi\psi^{i*}(\theta_i)\, dS, \tag{4.15a}$$

$$R = i(b\cos\theta_i)^{-1} \partial_\rho \int_D \chi\psi^{i*}(\pi - \theta_i)\, dS, \tag{4.15b}$$

$(\mathbf{r}, z)/(\boldsymbol{\rho}, \zeta)$ are suppressed in (4.14)/(4.15), and (as in §2) $\rho = a$ after carrying out the partial differentiations in (4.15).

5. Normal incidence

The subsequent development is restricted to normal incidence ($\theta_i = \beta = 0$) and $b < \lambda$ (so that only the dominant mode is propagated). $\mathbf{K}$, as given by (4.6), then may be reduced to

$$\mathbf{K} = -\frac{k^2}{2\pi}\Big[\sum_m I'_m(ka)\,K'_m(ka)\,e^{im(\theta-\alpha)} + \sum_l \sum_m I'_l(ka)\,I'_m(ka)\,S_{l+m}(kb)\,e^{-i(l\theta+m\alpha)}\cos\tfrac{1}{2}(l-m)\pi\Big], \tag{5.1}$$

where

$$S_m(z) = 2\sum_{n=1}^{\infty} K_m(nz) \tag{5.2}$$

is a Schlömilch series (see appendix A).† Combining the terms of corresponding positive and negative indices, we obtain the alternative form

$$\mathbf{K} = -\frac{k^2}{2\pi}\Big[\sum_{m=0}^{\infty} \epsilon_m I'_m(ka)\,K'_m(ka)\cos m(\theta-\alpha) + \frac{1}{2}\sum_{l=0}^{\infty}\sum_{m=0}^{\infty} \epsilon_l\,\epsilon_m\,I'_l(ka)\,I'_m(ka)\Big\{S_{l+m}(kb)\cos(l\theta+m\alpha)\cos\tfrac{1}{2}(l-m)\pi + S_{l-m}(kb)\cos(l\theta-m\alpha)\cos\tfrac{1}{2}(l+m)\pi\Big\}\Big], \tag{5.3}$$

where $\epsilon_0 = 1$ and $\epsilon_n = 2$ $(n = 1, 2, \ldots)$. The corresponding reductions of (4.11) and (4.15) yield (cf. Schwinger & Saxon 1968; Srokosz 1980)

$$\sum_n \mathbf{G}(\mathbf{r}; \boldsymbol{\rho}+n\mathbf{b}; k) = (2b)^{-1}\sum_{m=0}^{\infty} \epsilon_m (k^2+\nu_m^2)^{-\frac{1}{2}} \exp\{-(k^2+\nu_m^2)^{\frac{1}{2}}|x-\xi|\}\cos\{\nu_m(y-\eta)\} \quad (\nu_m = 2\pi m/b), \tag{5.4}$$

$$T = 1 + ib^{-1}\partial_\rho \int_D \chi(\alpha,\zeta)\,e^{i\kappa\rho\cos\alpha-\kappa\zeta}\,dS, \tag{5.5a}$$

$$R = ib^{-1}\partial_\rho \int_D \chi(\alpha,\zeta)\,e^{-i\kappa\rho\cos\alpha-\kappa\zeta}\,dS. \tag{5.5b}$$

We subsequently use (5.3) to calculate

$$H_{s,a} \equiv \operatorname{Re} K_{s,a} = \mathbf{F}^{-1}\{\operatorname{Re}\mathbf{K}_{s,a}\,Z_k(\zeta)\}, \tag{5.6}$$

where the subscript s/a signifies the symmetrical/antisymmetrical component, defined as in (2.19), but use (2.18) and (5.4) to calculate (note that the contribution of the continuous spectrum of $\mathbf{K}Z_k(\zeta)$ to its inverse transform K is real)

$$\operatorname{Im} K_{s,a} = -2\kappa\,e^{-\kappa(z+\zeta)}\partial_r\partial_\rho \operatorname{Im}\sum_n \mathbf{G}(\mathbf{r}; \boldsymbol{\rho}+n\mathbf{b}; \zeta) \tag{5.7a}$$

$$= b^{-1}\partial_r\partial_\rho \begin{Bmatrix}\cos\\ \sin\end{Bmatrix}(\kappa x)\begin{matrix}\cos\\ \sin\end{matrix}(\kappa\xi)\,e^{-\kappa(z+\zeta)}. \tag{5.7b}$$

† The greatly increased numerical difficulty of the solution for $\beta \neq 0$ stems principally from the appearance of the generalized Schlömilch series $S_m^{c,s}(z,\beta)$, obtained by inserting $\cos n\beta$, $\sin n\beta$ into (5.2), in the generalization of (5.1).

Substituting (5.6), (5.7) and

$$\psi^{\mathrm{i}}_{\mathrm{s,a}} = \left\{ \begin{matrix} \cos \kappa x \\ -i \sin \kappa x \end{matrix} \right\} e^{-\kappa z} \tag{5.8}$$

into the even and odd components of the integral equation (2.17), normalizing the symmetric and antisymmetric components of χ according to

$$\chi_{\mathrm{s}}(\theta, z) = \tfrac{1}{2}(T+R+1) f_{\mathrm{s}}(\theta, z), \quad \chi_{\mathrm{a}}(\theta, z) = \tfrac{1}{2} i (T-R+1) f_{\mathrm{a}}(\theta, z), \tag{5.9a,b}$$

and invoking (5.5), we obtain the reduced integral equations

$$\int_D H_{\mathrm{s}}(\theta, z; \alpha, \zeta) f_{\mathrm{s}}(\alpha, \zeta)\, dS = \kappa \sin(\kappa a \cos\theta) \cos\theta\, e^{-\kappa z}, \tag{5.10a}$$

$$\int_D H_{\mathrm{a}}(\theta, z; \alpha, \zeta) f_{\mathrm{a}}(\alpha, \zeta)\, dS = \kappa \cos(\kappa a \cos\theta) \cos\theta\, e^{-\kappa z}, \tag{5.10b}$$

where $z > h$ is implicit.

Combining (5.5) and (5.9), we obtain

$$i\left(\frac{T+R-1}{T+R+1}\right) = \frac{k}{b} \int_D f_{\mathrm{s}}(\alpha, \zeta) \sin(\kappa a \cos\alpha) \cos\alpha\, e^{-\kappa\zeta}\, dS \equiv \frac{1}{X_{\mathrm{s}}}, \tag{5.11a}$$

$$i\left(\frac{T-R-1}{T-R+1}\right) = \frac{k}{b} \int_D f_{\mathrm{a}}(\alpha, \zeta) \cos(\kappa a \cos\alpha) \cos\alpha\, e^{-\kappa\zeta}\, dS \equiv \frac{1}{X_{\mathrm{a}}} \tag{5.11b}$$

for the determination of R and T. Note that (5.6), (5.10) and (5.11) imply that $f_{\mathrm{s,a}}$ and $X_{\mathrm{s,a}}$ are real. Expressing T and R in terms of X_{s} and X_{a}, we obtain (after some reduction)

$$|T| = |\cos(\tau_{\mathrm{s}} - \tau_{\mathrm{a}})|, \quad |R| = |\sin(\tau_{\mathrm{s}} - \tau_{\mathrm{a}})|,$$

$$\arg T = \tfrac{1}{2}\pi + \arg R = \tau_{\mathrm{s}} + \tau_{\mathrm{a}}, \tag{5.12a,b,c}$$

where

$$\tau_{\mathrm{s,a}} = \tan^{-1}(1/X_{\mathrm{s,a}}). \tag{5.12d}$$

We remark that (5.12*a–c*) imply $|T|^2 + |R|^2 = 1$ and $|T \pm R| = 1$, as otherwise may be inferred directly from conservation of energy.

Multiplying (5.10*a,b*) through by $f_{\mathrm{s,a}}(\theta)$, integrating over the duct, dividing the results through by the square of the resulting integral on the left, and invoking (5.11*a,b*), we obtain the Schwinger-type variational representations

$$X_{\mathrm{s}} = \frac{b \int_D \int_D f_{\mathrm{s}}(\theta, z)\, H_{\mathrm{s}}(\theta, z; \alpha, \zeta) f_{\mathrm{s}}(\alpha, \zeta)\, d\theta\, dz\, d\alpha\, d\zeta}{\kappa^2 \left\{ \int_D f_{\mathrm{s}}(\theta, z) \sin(\kappa a \cos\theta) \cos\theta\, e^{-\kappa z}\, d\theta\, dz \right\}^2}, \tag{5.13a}$$

$$X_{\mathrm{a}} = \frac{b \int_D \int_D f_{\mathrm{a}}(\theta, z)\, H_{\mathrm{a}}(\theta, z; \alpha, \zeta) f_{\mathrm{a}}(\alpha, \zeta)\, d\theta\, dz\, d\alpha\, d\zeta}{\kappa^2 \left\{ \int_D f_{\mathrm{a}}(\theta, z) \cos(\kappa a \cos\theta) \cos\theta\, e^{-\kappa z}\, d\theta\, dz \right\}^2}, \tag{5.13b}$$

which are stationary with respect to variations of $f_{\mathrm{s,a}}(\theta, z)$ about the respective solutions of the integral equations (5.10*a,b*) and invariant under scale transformations of $f_{\mathrm{s,a}}$.

6. Surface-penetrating cylinders

If $h < 0$ the present problem is equivalent to that for an acoustical grating of circular cylinders or a circular piling in a wave tank. The contribution of the continuous spectrum $0 < k < \infty$ then vanishes, and $f_{s,a}$ admit the Fourier representations (both f_s and f_a must be even functions of θ by virtue of symmetry with respect to $y = 0$, which is a consequence of normal incidence)

$$f_s(z,\theta) = e^{-\kappa z} \sum_{n=0}^{N} A_{2n} \cos 2n\theta,$$

$$f_a(z,\theta) = e^{-\kappa z} \sum_{n=0}^{N} A_{2n+1} \cos(2n+1)\theta, \tag{6.1a,b}$$

where, in general, $N = \infty$ for an exact solution (but N for the truncated expansion of f_a need not be the same as that for f_s). Note that $A_0, A_1, A_2, A_3, \ldots$ are measures of the monopole, dipole, quadrupole, octupole, ... strengths of the grating.

Substituting (6.1a) and $H_s = 2\kappa \mathbf{H}_s \exp\{-\kappa(z+\zeta)\}$ into (5.13a), carrying out the integrations with respect to z and ζ, and invoking the identity

$$\sin(\kappa a \cos\theta)\cos\theta = \sum_{n=0}^{\infty} \epsilon_n (-)^{n-1} J'_{2n}(\kappa a) \cos 2n\theta \tag{6.2}$$

to evaluate the integral with respect to θ in the denominator of (5.13a), we obtain

$$X_s = \frac{\sum_{m=0}^{N}\sum_{n=0}^{N} X_{2m,2n} B_{2m} B_{2n}}{\left\{\sum_{n=0}^{N} (-)^n B_{2n}\right\}^2}, \quad B_n \equiv A_n J'_n(\kappa a), \tag{6.3a,b}$$

where, after suppressing the subscript on $\mathbf{H}$,

$$X_{mn} \equiv b\{2\pi^2 \kappa J'_m(\kappa a) J'_n(\kappa a)\}^{-1} \int_0^{2\pi}\int_0^{2\pi} \mathbf{H}(\theta;\alpha;i\kappa) \cos m\theta \cos n\alpha \, d\alpha \, d\theta. \tag{6.4}$$

Note that only the symmetrical/antisymmetrical component of $\mathbf{H} = \mathbf{H}_s + \mathbf{H}_a$ contributes to the integral in (6.4) if m and n are both even/odd.

The requirement that X_s be stationary with respect to variations of each of the A_{2n} yields $N+1$ linear algebraic equations, which may be inverted to obtain

$$A_{2m} J'_{2m}(\kappa a) = \lambda_s \sum_{n=0}^{N} (-)^n Y_{2m,2n}, \tag{6.5}$$

where λ_s is, in effect, a Lagrange multiplier (the variational representation of X_s is homogeneous in the B_n, and the variational problem may be reformulated to require the numerator of (6.3a) to be stationary with the side condition that the denominator be fixed), and the Y_{mn} are the elements of the inverse matrix

$$[Y_{2m,2n}] = [X_{2m,2n}]^{-1}. \tag{6.6}$$

The corresponding approximation to X_s is given by

$$X_s = \left\{\sum_{m=0}^{N}\sum_{n=0}^{N} (-)^{m+n} Y_{2m,2n}\right\}^{-1}. \tag{6.7}$$

The variational principle implies that the error in this approximation decreases monotonically with increasing N.

The constant λ_s may be determined by combining (6.1a), (6.3b) and (6.5) in (5.11a) and then invoking (6.7). The end result is

$$\lambda_s = -b/\pi a. \tag{6.8}$$

The corresponding results for A_{2n+1} and X_a may be obtained by replacing the even subscripts $2m$ and $2n$ by the odd subscripts $2m+1$ and $2n+1$ in (6.3a) and (6.5)–(6.7) and replacing λ_s by $\lambda_a = +b/\pi a$.

Substituting $\mathbf{H} = \mathrm{Re}\,\mathbf{K}$ from (5.3) into (6.4), carrying out the integrations with respect to α and θ, and expressing the modified Bessel functions I_n and K_n in terms of the Bessel functions J_n and Y_n, we obtain

$$X_{mn} = -\mu\{\delta_{mn} C_n + (-)^{\frac{1}{2}(m-n)} (D_{m+n} + D_{m-n})\}, \tag{6.9}$$

where δ_{mn} is the Kronecker delta,

$$\mu = \kappa b/2\pi = b/\lambda, \tag{6.10}$$

$$C_n \equiv C_n(\kappa a) = -\frac{\pi Y_n'(\kappa a)}{\epsilon_n J_n'(\kappa a)} \equiv \frac{\pi}{\epsilon_n} \cot \delta_n', \tag{6.11}$$

$$D_{2n} \equiv D_{2n}(\mu) = -\pi \sum_{m=1}^{\infty} Y_{2n}(2\pi m\mu) \equiv (-)^n \,\mathrm{Re}\, S_{2n}(-2i\pi\mu). \tag{6.12}$$

Note that $C_0 = O\{(\kappa a)^{-2}\}$ and $C_n = O\{(\kappa a)^{-2n}\}$ $(n \geqslant 1)$ as $\kappa a \downarrow 0$, and that m and n are either both even or both odd. The angles δ_n' are tabulated by Morse & Feshbach (1953, table XIV). The Schlömilch series $S_n(z)$ is considered further in appendix A.

Substituting (6.9) into (6.6), invoking (6.7) and its counterpart for X_a, and choosing $N = 1$, we obtain the second approximations

$$X_s = -\mu \left\{ \frac{(C_0+2D_0)(C_2+D_0+D_4)-4D_2^2}{(C_0+2D_0)+(C_2+D_0+D_4)-4D_2} \right\} \equiv X_s^{(2)}, \tag{6.13a}$$

$$X_a = -\mu \left\{ \frac{(C_1+D_0+D_2)(C_3+D_0+D_6)-(D_2+D_4)^2}{(C_1+D_0+D_2)+(C_3+D_0+D_6)-2(D_2+D_4)} \right\} \equiv X_a^{(2)}. \tag{6.13b}$$

The corresponding first approximations ($N = 0$)

$$X_s = -\mu(C_0+2D_0) \equiv X_s^{(1)}, \quad X_a = -\mu(C_1+D_0+D_2) \equiv X_a^{(1)} \tag{6.14a,b}$$

are plotted in figures 2(a, b). The first approximation to $|R|^2 = 1-|T|^2$, as determined from (5.12), is plotted in figure 3. The ratios $X_{s,a}^{(2)}/X_{s,a}^{(1)}$ are plotted in figure 4.

It is evident from figure 4 that the first approximations $X_{s,a}^{(1)}$ are likely to be adequate for $b < \frac{1}{2}\lambda$ and moderate values of $2a/b$ (which is likely to be small in practical configurations). That $X_s^{(2)}/X_s^{(1)}$ is larger than $X_a^{(2)}/X_a^{(1)}$ (in the parametric range considered here) is a consequence of the fact that the ratio of the quadrupole to monopole strengths is $O(\kappa^2 a^2)$ as $\kappa a \downarrow 0$, whereas the ratio of the octupole to dipole strengths is $O(\kappa^4 a^4)$; see comment following (6.12). Inspection of the known results for diffraction by a circular cylinder suggests that the error in the second approximations $X_{s,a}^{(2)}$ is less than 1 % for $\kappa a < 2$ provided that κb is not too close to 2π (note that, from the geometry of the problem, $\kappa a < \frac{1}{2}\kappa b$).

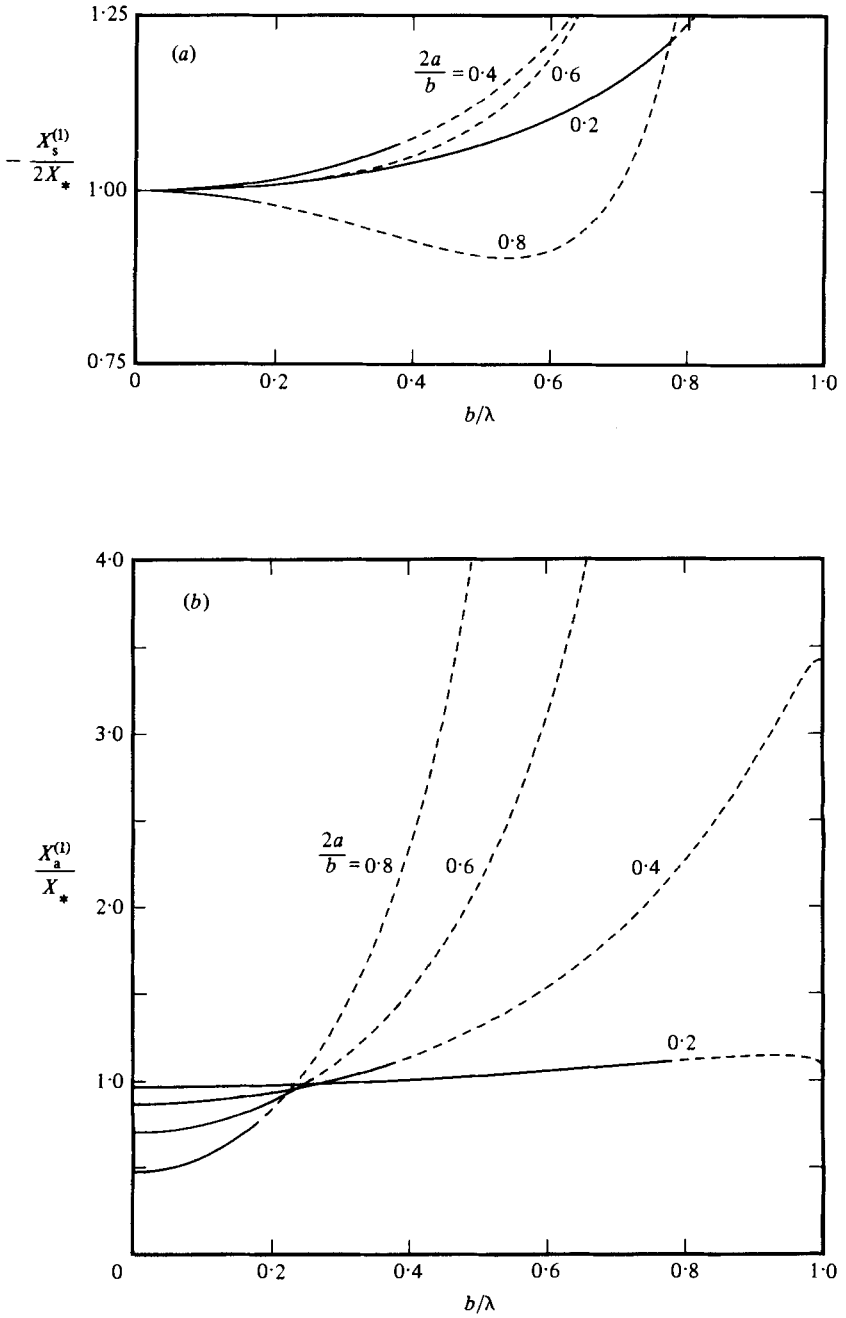

FIGURE 2. (*a*) $-X_s^{(1)}/2X_*$, as determined from (6.14*a*). Those segments for which $\kappa a > 0{\cdot}5$ (for which the approximation $X_s = X_s^{(1)}$ may be inadequate) are dashed. The curve for $2a/b = 0{\cdot}6$ and $\kappa a < 0{\cdot}5$ coincides (within the accuracy of the plot) with the curve for $2a/b = 0{\cdot}2$. (*b*) $X_a^{(1)}/X_*$, as determined from (6.14*b*). Those segments for which $\kappa a > 0{\cdot}5$ are dashed (but note that the approximation $X_a = X_a^{(1)}$ is better than $X_s = X_s^{(1)}$ and is likely to be adequate for $\kappa a < 1$).

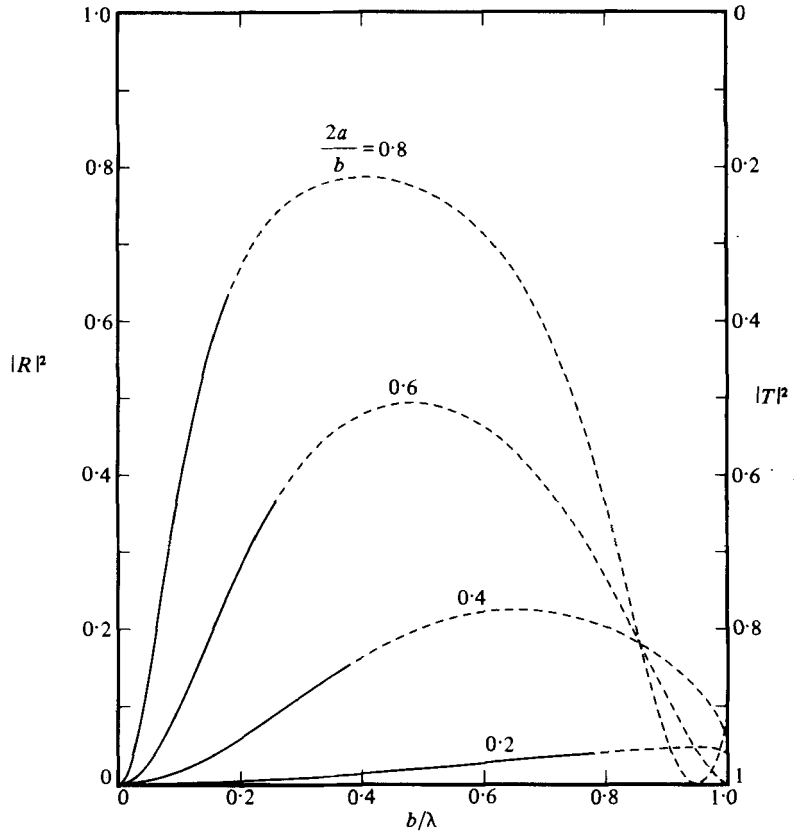

FIGURE 3. $|R|^2 = 1-|T|^2$ for $h = 0$, as determined from (5.12) using the approximations $X^{(1)}_{s,a}$. Those segments for which $\kappa a > 0{\cdot}5$ are dashed.

The limiting values of X_s and X_a as $a \downarrow 0$ with κ and b fixed are given by

$$X_s \to X_{00} \to -2X_*, \quad X_a \to X_{11} \to X_* \quad (a \downarrow 0, \quad h = 0), \tag{6.15a,b}$$

where

$$X_* \equiv b/\pi\kappa a^2 \tag{6.16}$$

is a convenient reference value. The limit (6.15a) is also valid for $\kappa a \downarrow 0$ with a/b fixed, but the corresponding limit of X_a depends on a/b. The second approximation (6.14b) yields

$$X^{(2)}_a \to X_* \left\{1-0{\cdot}8225(2a/b)^2-\frac{0{\cdot}0549(2a/b)^8}{1-0{\cdot}3179(2a/b)^6}\right\} \quad (\kappa a \downarrow 0, \quad h = 0). \tag{6.17}$$

The results in this section, which are basic for the subsequent development, are equivalent to those obtained by Twersky (1962), although he gives no numerical results.

7. Variational approximations for ducts

Returning to the original problem ($h > 0$), we posit the counterparts of (6.1) in the form

$$f_s(z,\theta) = \sum_{n=0}^{N} A_{2n} f_{2n}(z) \cos 2n\theta, \quad f_a(z,\theta) = \sum_{n=0}^{N} A_{2n+1} f_{2n+1}(z) \cos(2n+1)\theta, \tag{7.1a,b}$$

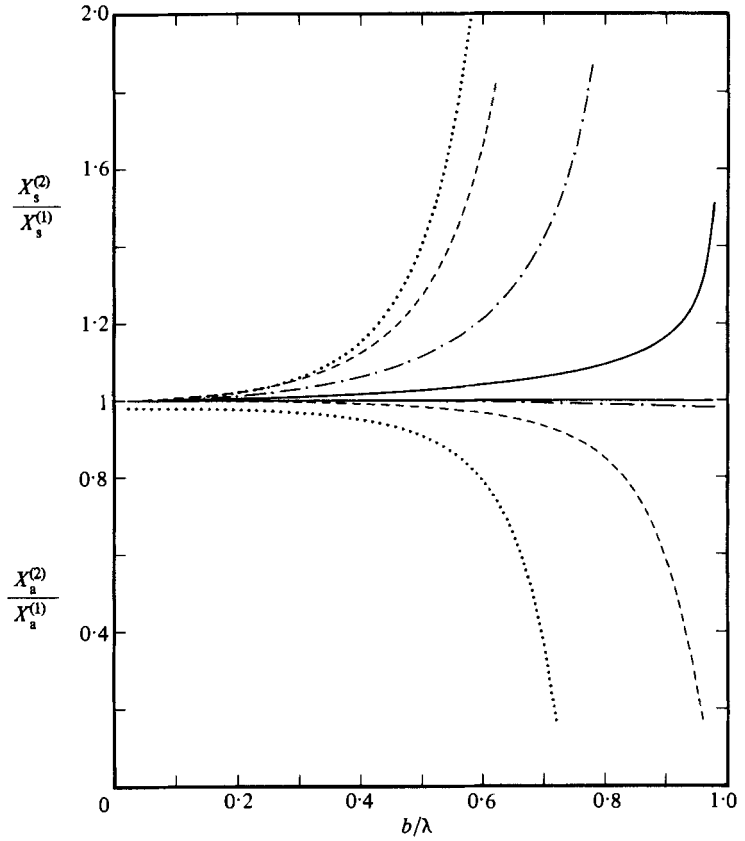

FIGURE 4. $X_s^{(2)}/X_s^{(1)}$ and $X_a^{(2)}/X_a^{(1)}$, as determined from (6.13a, b) and (6.14a, b), for $2a/b = 0{\cdot}2$ (——), $0{\cdot}4$ (—·—), $0{\cdot}6$ (– – –) and $0{\cdot}8$ (· · ·).

where $\{f_n(z)\}$ is a suitable set of functions (see below). Proceeding as in §6, we obtain

$$X_s = \frac{\sum_{m=0}^{N}\sum_{n=0}^{N} X_{2m,2n}\,\bar{A}_{2m}\,\bar{A}_{2n}}{\left\{\sum_{n=0}^{N}(-)^n\,\bar{A}_{2n}\right\}^2}, \quad \bar{A}_n = A_n\,F_n(i\kappa)\,J_n'(\kappa a) \tag{7.2a, b}$$

as the counterparts of (6.3a, b), where

$$F_n(k) = \int_h^\infty f_n(z)\,Z_k(z)\,dz, \tag{7.3}$$

$$X_{mn} = X_{mn}^{(0)} + \frac{b}{\pi^2\kappa^2 J_m'(\kappa a)\,J_n'(\kappa a)\,F_m(i\kappa)\,F_n(i\kappa)}\int_0^\infty \frac{F_m(k)\,F_n(k)\,M_{mn}(k)\,k^4\,dk}{k^2+\kappa^2}, \tag{7.4}$$

$X_{mn}^{(0)}$ is given by (6.9),

$$M_{mn}(k) = \frac{1}{2\pi k^2}\int_0^{2\pi}\int_0^{2\pi} \mathbf{H}(\theta;\alpha;k)\cos m\theta\cos n\alpha\,d\theta\,d\alpha = -\delta_{mn}\,\epsilon_n^{-1}\,I_n'(ka)\,K_n'(ka)$$
$$-\tfrac{1}{2}I_m'(ka)\,I_n'(ka)\{(-)^{\frac{1}{2}(m-n)}\,S_{m+n}(kb) + (-)^{\frac{1}{2}(m+n)}\,S_{m-n}(kb)\}, \tag{7.5}$$

and m and n are either both even or both odd in (7.5).

The counterparts of (6.5)–(6.8), which follow from the variational principle, are

$$A_{2m}\,F_{2m}(i\kappa)\,J'_{2m}(\kappa a) = -(2\pi\kappa a)^{-1}b\sum_{n=0}^{N}(-)^n\,Y_{2m,\,2n}, \tag{7.6}$$

$$[Y_{2m,\,2n}] = [X_{2m,\,2n}]^{-1}, \tag{7.7}$$

$$X_{\mathrm{s}} = \left\{\sum_{m=0}^{N}\sum_{n=0}^{N}(-)^{m+n}\,Y_{2m,\,2n}\right\}^{-1}, \tag{7.8}$$

whilst those for A_{2n+1} and X_{a} may be obtained by replacing the even subscripts $2m$ and $2n$ by the odd subscripts $2m+1$ and $2n+1$ in (7.2a) and (7.6)–(7.8) and changing the sign of the right-hand side of (7.6).

The preceding results may be generalized, to allow for more flexibility in the choice of trial functions, by replacing $A_{2n}f_{2n}$ in (7.1a) by $A^{\nu}_{2n}f_{\nu}$, where $\{f_{\nu}(z)\}$ is a suitable set of trial functions, and replacing the single summation over n by a double summation over n, ν. X_{mn} and Y_{mn} in (7.7) and (7.8) then must be replaced by $X^{\mu\nu}_{mn}$ and $Y^{\mu\nu}_{mn}$, where $X^{\mu\nu}_{mn}$ is obtained by replacing F_m and F_n in (7.4) by F_{μ} and F_{ν}, the matrices in (7.7) are then fourth order, and the double summation in (7.8) is replaced by a quadruple summation over m, n, μ, ν.

It remains to choose the $f_n(z)$, or, as proves expedient, the corresponding functions defined by the transformation (Simon 1981)

$$\hat{f}_n(z) = (\partial_z+\kappa)f_n(z), \tag{7.9}$$

the inverse of which, subject to the end condition $f_n(h) = 0$ (the pressure must be continuous at $z = h$), is

$$f_n(z) = \int_h^z e^{-\kappa(z-\zeta)}\hat{f}_n(\zeta)\,d\zeta, \tag{7.10}$$

and under which (7.3) goes over to

$$F_n(k) = \begin{cases} -k^{-1}\displaystyle\int_h^{\infty}\hat{f}_n(z)\sin kz\,dz \quad (0<k<\infty), \\[2ex] (2\kappa)^{-1}\displaystyle\int_h^{\infty}\hat{f}_n(z)\,e^{-\kappa z}\,dz \quad (k=ik). \end{cases} \tag{7.11}$$

Guided by the results for a deeply submerged, isolated duct (Miles 1982b) and invoking convenient normalizations, we choose

$$\hat{f}_0(z) = \kappa\{(\pi z_*)^{-\frac{1}{2}}e^{-z_*} + \mathrm{erf}\,z_*^{\frac{1}{2}}\}, \quad \hat{f}_n(z) = a^{-1}(\pi z_*)^{-\frac{1}{2}}e^{-nz_*} \quad (n\geqslant 1), \tag{7.12a,b}$$

where $z_* = (z-h)/a$. Note that (7.12a,b) imply the expected square-root singularity, $f\propto(z-h)^{\frac{1}{2}}$ as $z\to h$ and that

$$f_n \sim \delta_{0n} \quad (z_*\to\infty) \tag{7.13}$$

with exponentially vanishing remainders. Substituting (7.12) into (7.11), we obtain

$$F_0(k) = -\kappa k^{-2}\{[\tfrac{1}{2}(r+1)]^{\frac{1}{2}}\cos kh + [\tfrac{1}{2}(r-1)]^{\frac{1}{2}}\sin kh\}, \quad r = (1+k^2a^2)^{\frac{1}{2}}, \tag{7.14a}$$

$$F_n(k) = -(kr_n)^{-1}\{[\tfrac{1}{2}(r_n+n)]^{\frac{1}{2}}\sin kh + [\tfrac{1}{2}(r_n-n)]^{\frac{1}{2}}\cos kh\}, \quad r_n = (n^2+k^2a^2)^{\frac{1}{2}}, \tag{7.14b}$$

$$F_0(i\kappa) = \tfrac{1}{2}\kappa^{-1}(1+\kappa a)^{\frac{1}{2}}e^{-\kappa h}, \quad F_n(i\kappa) = \tfrac{1}{2}\kappa^{-1}(n+\kappa a)^{-\frac{1}{2}}e^{-\kappa h}. \tag{7.15a,b}$$

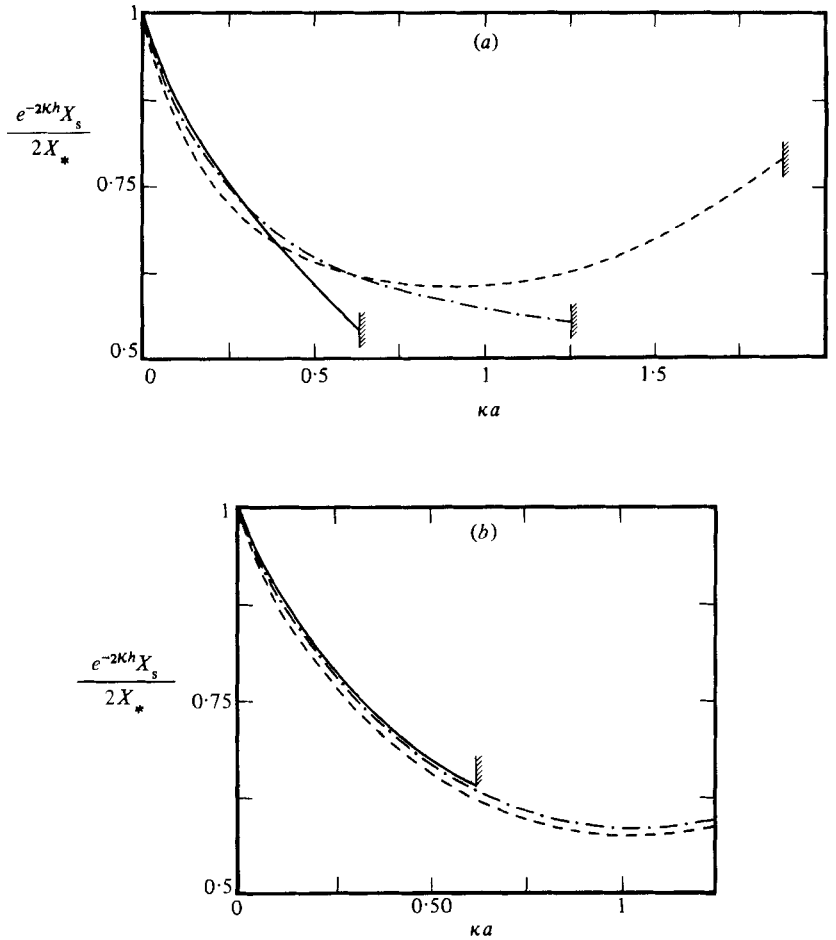

FIGURE 5. (*a*) $e^{-2\kappa h}X_s/2X_*$, as determined in §7, for $2a/b = 0{\cdot}2$ (——), $0{\cdot}4$ (—·—) and $0{\cdot}6$ (– – –) with $h/a = 1$. The cross-hatched lines correspond to $b = \lambda$. (*b*) As in (*a*), with $h/a = 4$.

The results for the acoustical grating suggest that truncation of (7.1*a*) at $N = 1$ (two terms) and (7.1*b*) at $N = 0$ (one term) should provide reasonable accuracy for $b < \lambda$. The corresponding approximations to X_s and X_a, as calculated from (7.8) and its odd counterpart, are plotted in figures 5(*a*, *b*) and 6(*a*, *b*).† The corresponding approximation to $|R|^2$ is less than 0·0014 in the parametric domains of figures 5 and 6. The inclusion of the additional trial function $\hat{f} = (h^2 - z^2)^{-\frac{1}{2}}$ for $n = 0$ was found to alter X_s by at most 0·2% in the parametric domain of figure 5. Note that X_s is relatively insensitive to a/b in the parametric domain of figure 5(*b*) and similarly for X_a in the parametric domains of figures 6(*a*, *b*); however, some resonance effects must be expected as $b/\lambda \to 1$.

† The numerical results presented here required many hours of computer time and various analytical and numerical devices for improving the convergence of the infinite integrals. It is possible that numerical solution of the integral equation(s) (5.10) – or, for oblique incidence, (2.17) – would be more efficient for extensive calculations; if so, the present results would provide important checks for such calculations.

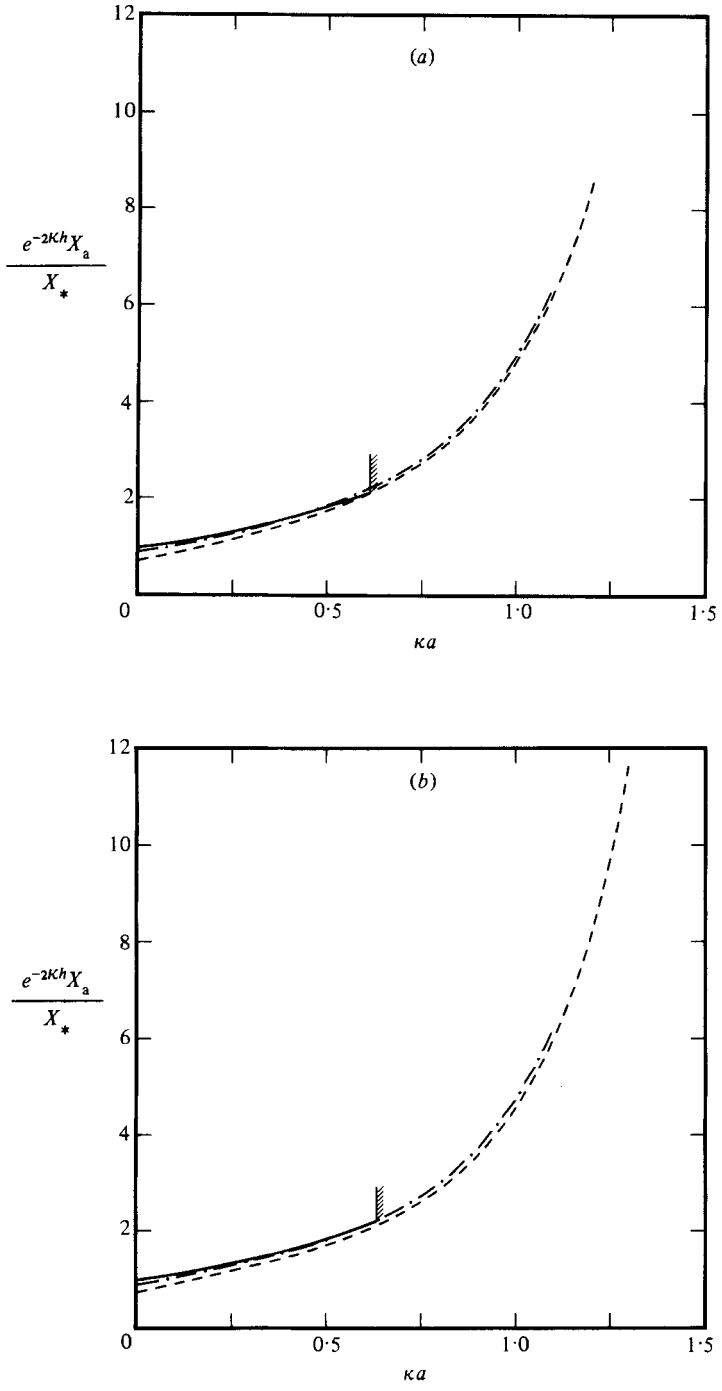

FIGURE 6. (*a*) $e^{-2\kappa h}X_a/X_*$, as determined in §7, for $2a/b = 0{\cdot}2$ (——), $0{\cdot}4$ (—·—) and $0{\cdot}6$ (– – –) with $h/a = 1$. The cross-hatched line corresponds to $b = \lambda$ for $2a/b = 0{\cdot}2$. (*b*) As in (*a*), with $h/a = 4$.

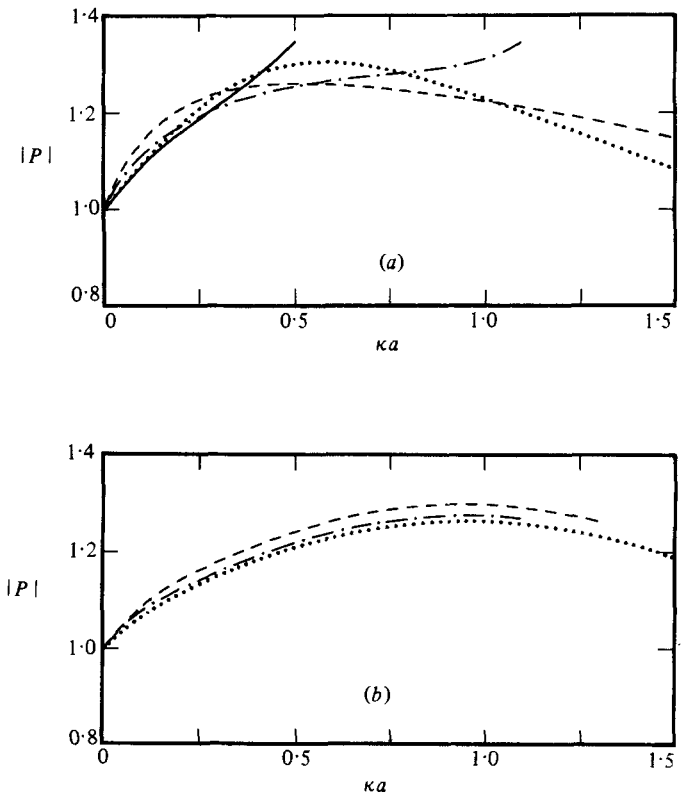

FIGURE 7. (*a*) $|P|$, as determined from (8.2*b*) using the results from §7, for $2a/b = 0{\cdot}2$ (——), $0{\cdot}4$ (—·—) and $0{\cdot}6$ (– – –), together with Simon's (1981) result for an isolated duct (· · ·), with $h/a = 1$. The concave-up portions of the curves for $2a/b = 0{\cdot}2$ and $0{\cdot}4$ presumably signal the approach to $b = \lambda$. (*b*) As in (*a*), with $h/a = 4$. The curve for $2a/b = 0{\cdot}2$ was found to be indistinguishable from the result for an isolated duct in $0 \leqslant \kappa a \leqslant 0{\cdot}5$.

8. Pressure-amplification factor

The amplification factor for any one of the ducts, defined as the ratio of the complex amplitude of the average pressure in the depths of the duct to that of the incident wave at the centre of the mouth (Knott & Flower 1980, in whose notation $P \equiv K$), is equal to that for the central ($n = 0$) duct, and is given by

$$P = (\pi a^2)^{-1} e^{\kappa h} \lim_{z\to\infty} \int_0^a \int_0^{2\pi} \psi(\mathbf{r}, z)\, r\, dr\, d\theta \tag{8.1a}$$

$$= e^{\kappa h} \lim_{z\to\infty} \psi(\mathbf{r}, z) \quad (r < a) \tag{8.1b}$$

$$= e^{\kappa h} \lim_{z\to\infty} \chi(\theta, z). \tag{8.1c}$$

Note that ψ must vanish as $z \to \infty$ in $r > a$ (the boundary conditions at $x = \pm\infty$ preclude a non-zero value of ψ in this limit) and, from (2.5*b*), must tend to a constant value as $z \to \infty$ in $r < a$, whence (8.1*c*) follows from (8.1*b*) and the definition of χ, (2.10)

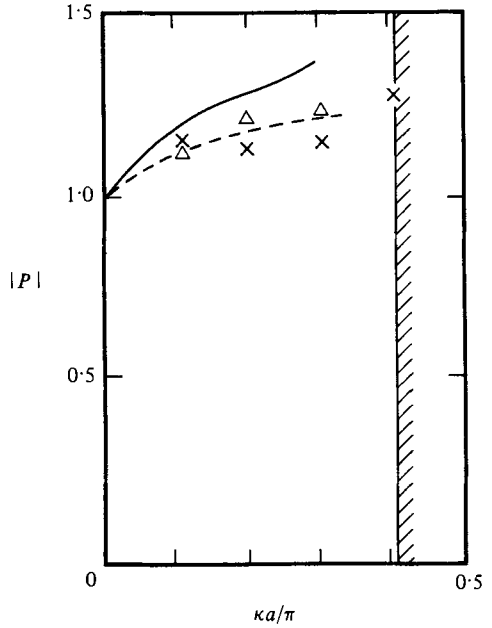

FIGURE 8. $|P|$, as determined from (8.2*b*) using the results from §7, compared with Knott & Flower's experimental values (△, ×) for $2a/b = 0{\cdot}41$ with $h/a = 0{\cdot}62$ (——, △) and $1{\cdot}34$ (– – –, ×). The cross-hatched line corresponds to $b = \lambda$ (there is a △ at $a/\pi = 0{\cdot}41$ and $|P| = 2{\cdot}2$).

with $n = 0$ therein. Relating $\chi(\theta, z)$ to $f(\theta, z)$ through (5.9) and (5.11) and invoking (7.1) and (7.13), we obtain

$$P = e^{\kappa h} \lim_{z \to \infty} \left\{ \left(\frac{X_s}{X_s + i} \right) f_s(z) + \left(\frac{X_a}{X_a + i} \right) f_a(z) \right\} \tag{8.2a}$$

$$= e^{\kappa h} \left(\frac{X_s}{X_s + i} \right) A_0. \tag{8.2b}$$

If, as proves to be true, $A_0 > 0$,

$$\arg P = -\tan^{-1} \frac{1}{X_s} \equiv -\tau_s. \tag{8.3}$$

It is shown in appendix B that $P \to 1$ as $\kappa a \to 0$ with b/a and h/a fixed.

The approximation obtained through the substitution of the results from §7 into (8.2*b*) is plotted in figures 7 (*a*, *b*) and also in figure 8, where it is compared with Knott & Flower's measurements. The corresponding approximation to $\arg P$ is plotted in figure 9.

Also plotted in figures 7 (*a*, *b*) is the result for a single duct, which, through a modification of the present formulation, is given by

$$P = 2e^{2\kappa h} \{\pi \kappa a (1 + \kappa a)^{\frac{1}{2}} J_1(\kappa a)\}^{-1} \left[\frac{2}{\kappa b} \hat{X}_s + i \right]^{-1}, \tag{8.4}$$

where $\hat{X}_s$ is calculated as above after setting $S_{m \pm n} = 0$ in (7.5) and $D_{m \pm n} = 0$ in (6.9); note that $(2/\kappa b)\, \hat{X}_s$ is independent of b. A comparison with Simon's numerical results (personal communication) suggests that the present approximation to $|P|$ is in error by about 5% for $h/a = 1$ and 1% for $h/a = 4$.

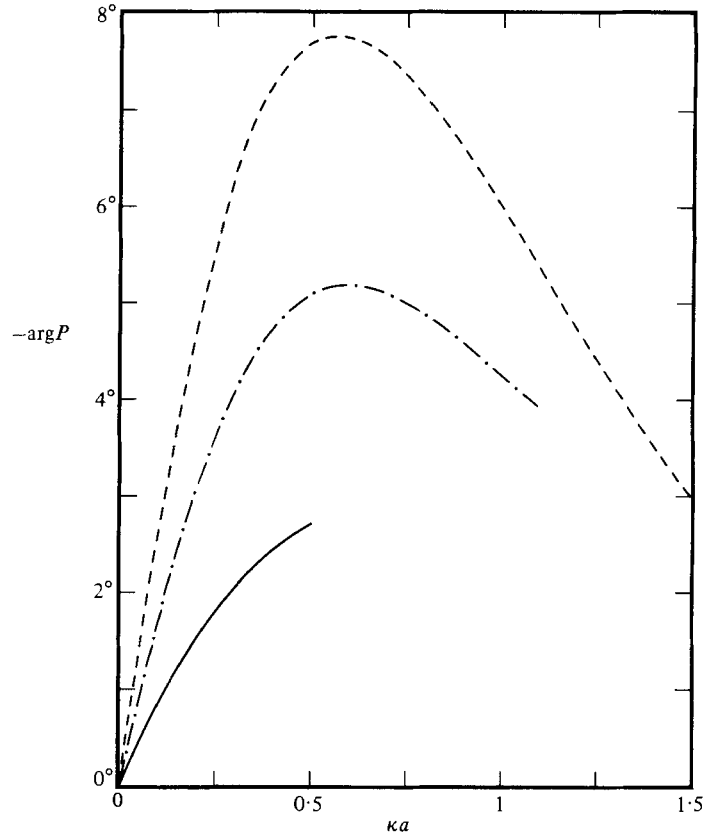

FIGURE 9. $-\arg P = \tau_s$, as determined from (8.3) using the results from §7, for $2a/b = 0{\cdot}2$ (——), $0{\cdot}4$ (— · —) and $0{\cdot}6$ (– – –) with $h/a = 1$. The corresponding values for $h/a = 4$, which may be calculated from the plots in figure 5(*b*), are smaller (in magnitude) than 1·5°.

9. Radiation problem

We turn now to the radiation problem for a duct in a wave tank (or, equivalently, a periodic row of ducts in which the forcing motions are in phase†) and for which the velocity potential may be posed in the form (cf. (2.3))

$$\phi(x,y,z,t) = \kappa^{-1}\,\mathrm{Re}\{Ve^{i\omega t}\psi(x,y,z)\}, \tag{9.1}$$

where V is the complex amplitude of the vertical velocity in the depths of the duct. The dimensionless complex potential ψ is symmetric with respect to $x = 0$ and satisfies (2.4), (2.5*a*),

$$\psi \sim (\Psi_0 - \kappa z)\,U(a-r) \quad (z \to \infty), \tag{9.2}$$

where U is the unit step function [$U(x) = 0, 1$ for $x \lessgtr 0$], (2.6) at $r = a$ ($n = 0$), and the radiation condition ($b < \lambda$ throughout this section)

$$\psi \sim \Psi_1 e^{-i\kappa|x|-\kappa z} \quad (\kappa x \to \pm\infty). \tag{9.3}$$

The complex parameters Ψ_0 and Ψ_1 are to be determined.

† The present formulation admits an obvious generalization to radiation from a periodic row of ducts in which the forcing motion exhibits an interduct phase shift of the form $\exp(-in\beta)$, as in (2.9*a*) and (2.14).

The impedance of the duct, defined as the ratio of the complex amplitude of the perturbation pressure to that of the vertical velocity (positive up) in the depths of the duct, is $\mathbf{Z} = i\rho\omega(z-\kappa^{-1}\Psi_0)$ (Miles 1982*a*), where ρ is the fluid density. The corresponding impedance for the motion in $r < a$, regarded as independent of the motion in $r > a$, is $\mathbf{Z}_< = i\rho\omega(z-\kappa^{-1})$, whence the radiation impedance is

$$\mathbf{Z}_> \equiv \mathbf{Z}-\mathbf{Z}_< = i\rho c(1-\Psi_0), \tag{9.4}$$

where $c = \omega/\kappa$ is the phase speed of the radiated wave. The real and imaginary parts of $\mathbf{Z}_>$, the radiation resistance $\rho c \operatorname{Im}\Psi_0$ and the radiation reactance $\rho c(1-\operatorname{Re}\Psi_0)$, are measures of the radiation damping and virtual mass (or virtual stiffness if $\operatorname{Re}\Psi_0 > 1$) of the fluid in $r > a$; $i\rho c$ is the impedance of the radiated wave.

The requirement that the energy flux through the duct be equal to that of the radiated waves at $x = \pm\infty$ yields (after a straightforward calculation)

$$\operatorname{Im}\Psi_0 = X_*|\Psi_1|^2, \tag{9.5}$$

where $X_* = b/\pi\kappa a^2$, as in (6.16); (9.5) also may be obtained by applying Green's second theorem to ψ and its complex conjugate (cf. Simon 1981). Similarly, Ψ_1 may be related to P, the pressure-amplification factor for the diffraction problem, by applying Green's theorem to the solutions of the (normal-incidence) diffraction and radiation problems (cf. Srokosz 1980; Simon 1981). The end result is

$$\Psi_1 = iX_*^{-1}\, e^{-\kappa h}\, P, \tag{9.6}$$

which may be combined with (9.5) to obtain

$$\operatorname{Im}\Psi_0 = X_*^{-1}\, e^{-2\kappa h}\, |P|^2. \tag{9.7}$$

The solution of (2.4), (2.5*a*), (2.6), (9.2) and (9.3) may be posed in the form (cf. (2.15))

$$\psi = U(a-r)\, Z_0(z) + \partial_\rho \left\{ \int_A Z_0(\zeta) - \int_D \chi(\alpha,\zeta) \right\} \sum_n G_s(\mathbf{r}, z; \boldsymbol{\rho}+n\mathbf{b}, \zeta)\, dS, \tag{9.8}$$

where (cf. (3.1))

$$Z_0(z) = 1-\kappa z, \tag{9.9}$$

$U(a-r)\, Z_0(z)$ describes the motion in $r < a$, regarded as independent of the motion in $r > a$, $\chi + Z_0$ is the jump in ψ across the duct wall ($r = a$, $z > h$), defined as in (2.10), $\int_D$ signifies integration over the duct, as in (2.16), $\int_A$ signifies the corresponding integration over the aperture ($\rho = a$, $0 < \zeta < h$), and G_s is the symmetrical part of the Green function developed in §4; note that, by construction, ψ is continuous across the aperture. Letting $x \uparrow \infty$ in (9.8), using (5.4) to obtain the asymptotic form of $\Sigma_n G_s$, and comparing the result with (9.3), we obtain

$$\Psi_1 = i\kappa b^{-1} \left\{ \int_A Z_0(\zeta) - \int_D \chi(\alpha,\zeta) \right\} e^{-\kappa\zeta} \sin(\kappa a \cos\alpha) \cos\alpha\, dS. \tag{9.10}$$

Separating the real and imaginary parts of $\Sigma_n G_s$, the latter being determined by (4.11), in (9.8) and invoking (9.10), we obtain

$$\psi = U(a-r)\, Z_0(z) + \Psi_1 \cos\kappa x\, e^{-\kappa z} + \partial_\rho \left\{ \int_A Z_0(\zeta) - \int_D \chi(\alpha,\zeta) \right\}$$

$$\times \operatorname{Re} \sum_n G_s(\mathbf{r}, z; \boldsymbol{\rho}+n\mathbf{b}, \zeta)\, dS. \tag{9.11}$$

The boundary condition (2.6) then yields the integral equation

$$\int_D H_s(\theta, z; \alpha, \zeta)\, \chi(\alpha, \zeta)\, dS = \kappa \Psi_1 \sin(\kappa a \cos\theta) \cos\theta\, e^{-\kappa z} + \int_A H_s(\theta, z; \alpha, \zeta)\, Z_0(\zeta)\, dS \quad (z > h), \tag{9.12}$$

where H_s is defined by (5.6).

A variational formulation does not appear to offer any significant advantage in the present problem; accordingly, we attack (9.12) directly by Galerkin's method. Comparing (9.12) with (5.10a), we infer that χ must be a linear superposition of $\Psi_1 f_s$ and a component that is forced by the second term on the right-hand side of (9.12); moreover, the latter component is real (χ is complex because Ψ_1 is complex, but H_s and Z_0 are real). Guided by this consideration, by symmetry, and by the requirements $\chi = -Z_0 = \kappa h - 1$ at $z = h$ (where the pressure jump $\chi + Z_0$ must vanish) and $\chi = O(1)$ as $z \to \infty$, we pose the solution of (9.12) in the form

$$\chi(\theta, z) = \kappa h - 1 + \sum_n (\Psi_1 A_{2n} + B_{2n}) f_{2n}(z) \cos 2n\theta, \tag{9.13}$$

where the A_{2n} and $f_{2n}(z)$ are defined as in §7 (but see below). Substituting (9.13) into (9.12), separating out the terms in Ψ_1, which cancel by virtue of (5.10a) and (7.1a), multiplying the remaining result through by $f_{2m}(z) \cos 2m\theta$, invoking $H_s = \mathbf{F}^{-1}\{\mathbf{H}_s Z_k(\zeta)\}$, (6.4), (7.4) and (7.5$a$), and integrating over the duct, we obtain the linear algebraic set

$$\sum_n X_{2m,2n} C_{2n} = X_{2m*}, \quad C_n = B_n \frac{F_n(i\kappa) J_n'(\kappa a)}{F_*(i\kappa) J_0'(\kappa a)}, \tag{9.14a,b}$$

where X_{mn} is given by (7.4), and X_{m*} is given by (7.4) after replacing J_n' by J_0' and $F_n(k)$ and $F_n(i\kappa)$ by

$$F_*(k) = -\kappa k^{-2} Z_k(h), \quad F_*(i\kappa) = \kappa^{-1} e^{-\kappa h}. \tag{9.15a,b}$$

It should be remarked that $B_{2n} f_{2n}(z)$ in (9.13) could be replaced by $B_{2n} g_{2n}(z)$, where $\{g_n(z)\}$ is a set of expansion functions that must satisfy the same basic conditions as, but may differ from, $\{f_n(z)\}$, in which case X_{mn} in (9.14) would be obtained by replacing F_m and F_n in (7.4) by G_m and G_n, and X_{m*} would be obtained by replacing F_m by G_m and F_n by F_*. Further generalization could be effected along the lines of the paragraph following (7.8).

The limiting value of $\chi + Z_0$ as $z \to \infty$ must be given by (9.2), whence (cf. §8)

$$\Psi_0 = 1 + \chi_0(\infty), \tag{9.16}$$

where $\chi_0(z)$ is the axisymmetric component of $\chi(\theta, z)$. Substituting (9.13) into (9.16) and invoking (7.13), we obtain

$$\Psi_0 = \kappa h + \Psi_1 A_0 + B_0. \tag{9.17}$$

Expressing Ψ_1 and A_0 in terms of P with the aid of (9.6) and the complex conjugate of (8.2b), respectively, substituting $B_0 = 2C_0(1+\kappa a)^{-\frac{1}{2}}$ from (9.14b), (7.15a) and (9.15b), and separating the real and imaginary parts of Ψ_0, we obtain (9.7) and

$$\operatorname{Re} \Psi_0 = \kappa h + 2C_0(1+\kappa a)^{-\frac{1}{2}} + (X_* X_s)^{-1} e^{-2\kappa h} |P|^2. \tag{9.18}$$

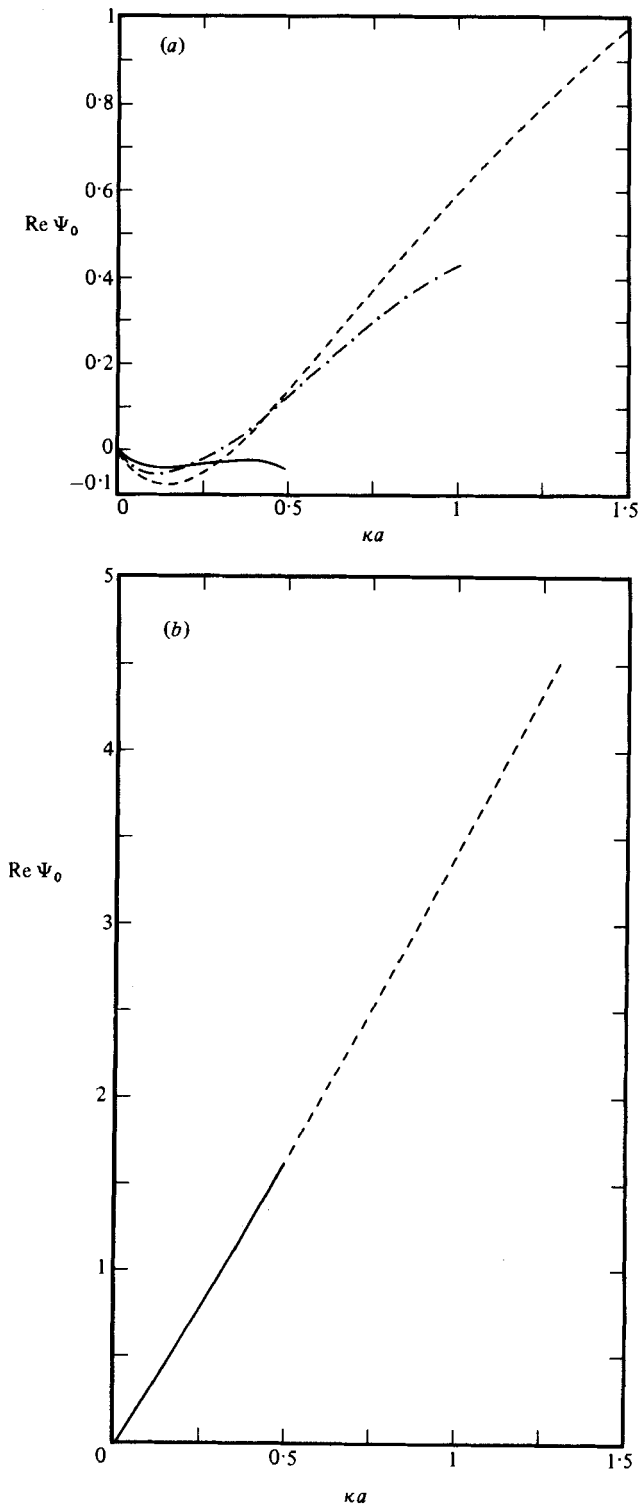

FIGURE 10. (*a*) $\mathrm{Re}\,\Psi_0$, as determined in §9, for $2a/b = 0{\cdot}2$ (——), $0{\cdot}4$ (— · —) and $0{\cdot}6$ (– – –) with $h/a = 1$. (*b*) As in (*a*), with $h/a = 4$. The results for $2a/b = 0{\cdot}2$ and $0{\cdot}4$ are indistinguishable from those for $2a/b = 0{\cdot}6$ in $\kappa a < 0{\cdot}5$ and $1{\cdot}2$ respectively.

The approximation to $\mathrm{Re}\,\Psi_0$ obtained by including the first two terms ($2n = 0, 2$) in the Fourier series in (9.13) and using the trial functions (7.12a, b) for $n = 0, 2$ is plotted in figure 10. The corresponding approximation to $\mathrm{Im}\,\Psi_0$ may be obtained by substituting $|P|$ from §8 into (9.7).

The solution of the integral equation (9.12) in the limit $\kappa a \downarrow 0$ may be obtained by the procedure outlined in appendix B for the solutions of (5.10a, b). The end results are

$$\chi = \kappa h - 1 + iX_*^{-1} e^{-2\kappa h}\{1 - e^{-\kappa(z-h)}\}, \tag{9.19}$$

$$\Psi_0 = \kappa h + iX_*^{-1} e^{-2\kappa h}, \quad \Psi_1 = iX_*^{-1} e^{-\kappa h} \tag{9.20a, b}$$

within error factors of $1 + O(\kappa^2 a^2)$ for each of the real and imaginary parts.

This work was supported in part by the Physical Oceanography Division, National Science Foundation, NSF Grant OCE77-24005, and by a contract with the Office of Naval Research.

Appendix A. Schlömilch series

The Schlömilch series

$$S_n(z) = 2\sum_{l=1}^{\infty} K_n(lz) \tag{A 1}$$

converges exponentially for real values of z, but convergence is slow for small z and is only conditional for imaginary z. More rapidly converging forms for small or imaginary z are given by

$$S_0(z) = \pi z^{-1} + \ln\frac{\gamma z}{4\pi} + \mathbf{F}_0\left(\frac{iz}{2\pi}\right) \tag{A 2}$$

(Twersky 1961), where $\ln\gamma = 0{\cdot}577\ldots$ is Euler's constant,

$$\mathbf{F}_0(x) = \sum_{m=1}^{\infty}\{(m^2 - x^2)^{-\frac{1}{2}} - m^{-1}\} \tag{A 3a}$$

$$= 0{\cdot}601x^2 + 0{\cdot}389x^4 + 0{\cdot}315x^6 + \ldots, \tag{A 3b}$$

and†

$$S_{2n}(z) = (-)^n\left\{\frac{\pi}{z} - \frac{1}{2n} - \sum_{m=1}^{n}\frac{2^{2m-1}(n+m-1)!\,B_{2m}}{(2m)!\,(n-m)!}\left(\frac{2\pi}{z}\right)^{2m}\right\} + \mathbf{F}_{2n}\left(\frac{iz}{2\pi}\right) \quad (n \geqslant 1); \tag{A 4}$$

B_{2n} are the Bernoulli numbers ($B_2 = \frac{1}{6}$, $B_4 = -\frac{1}{30}$, $B_6 = \frac{1}{42}$, ...) and

$$\mathbf{F}_n(x) = \sum_{m=1}^{\infty}\frac{\{m - (m^2 - x^2)^{\frac{1}{2}}\}^n}{x^n(m^2 - x^2)^{\frac{1}{2}}} \quad (n \geqslant 1) \tag{A 5a}$$

$$= \zeta(n+1)\,(\tfrac{1}{2}x)^n + (n+2)\,\zeta(n+3)\,(\tfrac{1}{2}x)^{n+2} + \ldots, \tag{A 5b}$$

where $\zeta(n)$ is Riemann's zeta function.

Appendix B. The limit $\kappa a \downarrow 0$

Letting $ka \downarrow 0$ with $kb = O(1)$ in (5.13), we obtain

$$\mathbf{K} = \sum_{m=0}^{\infty}\mathbf{K}_m \cos m(\theta - \alpha), \tag{B 1}$$

$$\mathbf{K}_0 = (4\pi)^{-1}k^2, \quad \mathbf{K}_m = (2\pi a^2)^{-1}m \quad (m \geqslant 1), \tag{B 2a, b}$$

† $S_{2n}(z) = \frac{1}{2}i\pi(-)^n H_{2n}(iz/2\pi)$ in Twersky's (1961) notation. The particular result considered here was obtained originally by Ignatowsky; see Twersky (1961) for references.

where, here and subsequently, $k = O(\kappa)$, and error factors of $1+O(\kappa^2 a^2)$ are implicit. Invoking (5.6) to obtain H_s and H_a, substituting the results into (5.10a, b), letting $\kappa a \downarrow 0$, introducing

$$f_s = \sum_{n=0}^{\infty} f_{2n}(z)\cos 2n\theta, \quad f_a = \sum_{n=0}^{\infty} f_{2n+1}(z)\cos(2n+1)\theta, \tag{B 3a,b}$$

$$F_n(k) = \int_h^{\infty} f_n(z)\, Z_k(z)\, dz \tag{B 4}$$

((B 3a, b) and (B 4) are equivalent to (7.1a, b) and (7.3) after absorbing the A_n in the $f_n(z)$), and equating coefficients of $\cos m\theta$ for $m = 0, 1, 2$, we obtain

$$\kappa^2 e^{-\kappa z} = \mathbf{F}^{-1}\{k^2 F_0(k)\} = -f_0''(z), \tag{B 5a}$$

$$\kappa e^{-\kappa z} = \tfrac{1}{2}a^{-1}\mathbf{F}^{-1}\{F_1(k)\} \equiv \tfrac{1}{2}a^{-1}f_1(z), \tag{B 5b}$$

$$\kappa^2 e^{-\kappa z} = 2a^{-2}\mathbf{F}^{-1}\{F_2(k)\} \equiv 2a^{-2}f_2(z), \tag{B 5c}$$

where, here and subsequently, $z > h$ is implicit. The corresponding results for $m > 2$ are not significant within the present approximation.

Integrating (B 5a) and requiring f_0 to vanish at $z = h$ (since ψ must be continuous) and to be finite at $z = \infty$, we obtain

$$f_0(z) = e^{-\kappa h} - e^{-\kappa z}, \tag{B 6a}$$

whilst (B 5b, c) imply

$$f_1(z) = 2\kappa a\, e^{-\kappa z}, \quad f_2(z) = \tfrac{1}{2}(\kappa a)^2 e^{-\kappa z}. \tag{B 6b,c}$$

These limiting results are not uniformly valid near $z = h$, where $f_n(z)$ is singular like $(z-h)^{\frac{1}{2}}$. This non-uniformity is more serious for f_1 and f_2, which, in contrast to f_0, do not vanish at $z = h$ and therefore imply (physically unacceptable) discontinuities in the dipole and quadrupole components of ψ.

The corresponding limits for X_s and X_a, obtained through (5.15a, b), are

$$X_s = 2X_* e^{2\kappa h}, \quad X_a = X_* e^{2\kappa h}. \tag{B 7a,b}$$

We remark that (B 7a) is the negative of (6.15a), whereas (B 7b) is equal to (6.15b), in the singular limit $\kappa h \downarrow 0$.

A similar analysis may be carried out for $\kappa a \to 0$ with $b = O(a)$. The results (B 6a) and (B 7a) remain unchanged, although the implicit error factor $1+O(\kappa^2 a^2)$ becomes $1+O(\kappa^2 a^2, \kappa a^2/b)$; (B 6$b, c$) and (B 7$b$) are found to contain factors that depend on a/b and tend to unity as $a/b \to 0$; cf. (6.17).

Combining (B 6a) and (B 7a) in (8.1c), we obtain

$$P \to 1 \quad \left(\kappa a \downarrow 0; \quad \frac{b}{a}, \frac{h}{a} \text{ fixed}\right), \tag{B 8}$$

which generalizes Simon's (1981) result for an isolated duct.

REFERENCES

Evans, D. V. 1981 Power from water waves. *Ann. Rev. Fluid Mech.* **13**, 157–187.

Falnes, J. & Budal, K. 1982 Wave-power absorption by parallel rows of interacting bodies. *Appl. Ocean Res.* (to be published).

Havelock, T. H. 1929 Forced surface waves on water. *Phil. Mag.* **8**(7), 569–576.

Knott, G. F. & Flower, J. O. 1980 Wave-tank experiments on an immersed vertical circular duct. *J. Fluid Mech.* **100**, 225–236.

LIGHTHILL, J. 1979 Two-dimensional analyses related to wave-energy extraction by submerged resonant ducts. *J. Fluid Mech.* **91**, 253–317.

MAGNUS, W., OBERHETTINGER, F. & SONI, R. P. 1966 *Formulas and Theorems for the Special Functions of Mathematical Physics.* Springer.

MILES, J. W. 1982*a* On surface-wave radiation from a submerged cylindrical duct. *J. Fluid Mech.* **122**, 339–346.

MILES, J. W. 1982*b* Surface-wave interaction with a deeply submerged circular duct. *J. Austral. Math. Soc.* (to be published).

MORSE, P. M. & FESHBACH, H. 1953 *Methods of Theoretical Physics.* McGraw-Hill.

SCHWINGER, J. S. & SAXON, D. S. 1968 *Discontinuities in Waveguides*, pp. 26, 27. Gordon & Breach.

SIMON, M. J. 1981 Wave-energy extraction by a submerged cylindrical resonant duct. *J. Fluid Mech.* **104**, 159–187.

SIMON, M. J. 1982 Multiple scattering in arrays of axisymmetric wave-energy devices. Part 1. A matrix method using a plane-wave approximation. *J. Fluid Mech.* **120**, 1–25.

SROKOSZ, M. A. 1980 Some relations for bodies in a canal with reference to wave-power absorption. *J. Fluid Mech.* **99**, 145–162.

THOMAS, J. R. 1981 The absorption of wave energy by a three-dimensional submerged duct. *J. Fluid Mech.* **104**, 189–215.

TWERSKY, V. 1961 Elementary function representations of Schlömilch series. *Arch. Rat. Mech. Anal.* **8**, 323–332.

TWERSKY, V. 1962 On scattering of waves by the infinite grating of circular cylinders. *IEEE Trans. on Antennas and Propagation* **10**, 737–765.

WATSON, G. N. 1945 *A Treatise on the Theory of Bessel Functions.* Cambridge University Press.